Hindawi
Advances in Mathematical Physics
Volume 2021, Article ID 5598817, 11 pages
https://doi.org/10.1155/2021/5598817

Research Article

Optimal Homotopy Asymptotic Method for Investigation of Effects of Thermal Radiation, Internal Heat Generation, and Buoyancy on Velocity and Heat Transfer in the Blasius Flow

Dachas Ibrahim, Mitiku Daba, and Solomon Bati

Department of Mathematics, Jimma University, Jimma, Oromia, Ethiopia

Correspondence should be addressed to Solomon Bati; solomonbati@yahoo.com

Received 26 February 2021; Revised 10 April 2021; Accepted 13 May 2021; Published 31 May 2021

Academic Editor: Yannis Dimakopoulos

In this study, analytical examination of effects of internal heat generation, thermal radiation, and buoyancy force on flow and heat transfer in the Blasius flow over flat plate has been presented. The governing nonlinear partial differential equations of the problem are transformed into a set of coupled nonlinear third-order ordinary differential equations by the similarity variable method and have been systematically solved using the optimal homotopy asymptotic method. The main aim of the present study is to inspect the effects of various physical parameters in the flow model on velocity and heat transfer in steady two-dimensional laminar boundary layer flow with convective boundary conditions. The influences of the Grashof number, internal heat generation, the Biot number, radiation parameter, and the Prandtl number on the skin-friction coefficient, the fluid velocity profile, and temperature distribution have been determined and discussed in detail through several plots. The finding revealed that the fluid velocity and temperature delivery upsurge with snowballing in the values of the Biot number and internal heat generation parameters. The temperature profile of the fluid declines contrary to the value of the Grashof number and the Prandtl number but increases with thermal radiation. Moreover, it is found that the skin-friction coefficient and the rate of heat intensify with the Grashof number, internal heat generation, the Biot number, and thermal radiation parameter. The obtained result is likened with the previously published numerical results in a limited case of the problem and shows an excellent agreement.

1. Introduction

The term boundary layer flow refers to a type of flow in a comparatively narrow region nearby a solid surface where the influence of viscosity is considerable. The study of boundary layer flow and its applications are important for development in the field of applied science, engineering, and technology. The Blasius boundary layer designates an incompressible 2D laminar boundary layer that forms on a semi-infinite plate apprehended in parallel to a continuous omnidirectional flow. Flow of incompressible viscous fluid and heat transfer phenomena over stretching sheets has plentiful practical application in the field of science and engineering, in the chemical and manufacturing process like aerodynamics, extrusion of plastic sheets, continuous casting of metals, glass fibers, and paper production. Blasius [1] was the first investigator who studied boundary layer flow regarding a stationary plate. He applied a similarity transformation technique in order to reduce the Navier Stoke equation for the viscid incompressible steady laminar flow from PDE to ODE and introduces the laminar boundary layer equation known as the Blasius equation. Blasius solved the famous boundary layer equation for a flat moving plate problem and found a power series solution of the model. Afterward, it has been expanded by many researchers [2–5] to explore the similar solutions for the thermal physical phenomenon flows over a flat plate under different flow configurations and boundary conditions. Abussita [6] studied the solution of the Blasius equation for the mixing layers of fluid past a flat plate and establish the existence of a solution. Falkner and Skan [7] generalized the Blasius problem by considering the physical phenomenon flow over a wedge inclined at a specific angle. Wang [8] used the Adomian decomposition method for the approximate solution of the classical Blasius problem.

Reddy et al. [9] develop a mathematical model of heat transfer augmentation in the Blasius-Rayleigh-Stokes flow through a heated moving plate by implementing the Cattaneo–Christov heat flux model and transitive magnetic field. They used similarity transformation to convert dimensional quantity into a dimensionless form to solve the problem numerically and discuss the influence of embedded parameters on velocity and temperature of the fluid.

Heat transfer is a dynamic process in which internal energy is transferred naturally from one material to another. It is very vital to study the impact of heat transfer in various materials and boundary layer flows over stretching sheet because of their substantial applications in numerous biological phenomena, engineering, and industrial process like paper production, metal extrusion, fermentation, bubble absorption, evaporators, condensers, and air conditioning systems [10]. The key concern of heat transfer study is to avert the heat loss in important industrial processes. Heat transfer in the laminar boundary layer flow over a stretching sheet with thermal radiation effect has several industrial applications, including combustion, furnace design, nuclear reactor safety, fluidized bed heat exchangers, solar collectors, turbid water bodies, and photochemical reactors [11]. Thermal radiation can be used to attain the required heat transfer rate accompanied by the temperature distribution in the boundary layer region. For this reason, the effects of radiation are very important in various application areas like soil physics, geothermal energy extraction, chemical engineering, glass production, furnace design, space technology application, power generation systems, fight aerodynamics, and plasma physics which operate at extremely high temperature. In view of these applications, recently, many authors [12, 13] studied the effect of various pertinent physical parameters on flow and heat transfer of Newtonian and non-Newtonian fluids flow over a surface as well as a disk by considering various flow situations and boundary conditions and achieved very essential results.

Mabood and Waqar [14] studied the consequences of radiation on heat transfer from a horizontal plane in an exceedingly two-dimensional, incompressible steady, and viscous flow using OHAM. Reddy et al. [15] examined the Darcy-Forchheimer two-dimensional carbon nanotubes flow in light of a melting surface with warm nonlinear radiation, Cattaneo–Christov heat flux, and slip condition. They investigated the impacts of various constraints on various profiles, and they found that velocity and corresponding thickness of the boundary layer declines for rising values of the Forchheimer parameter and porosity parameter. Moreover, inclined values of melting parameter display a diminishing pattern for the temperature field. Kuo [16] has provided the solution of thermal boundary layer problems for flow past flat plates using the differential transform method. Sakiadis [17] investigated the boundary layer flow over a continuously moving rigid surface with a continuing speed. Crane [18] investigated the boundary layer flow due to a stretching surface and discovered the precise solutions of the boundary layer equations.

Convective heat transfer with radiation study is incredibly essential with the process involving high temperatures like atomic power plants, gas turbines, and thermal energy storage. In light of those numerous applications, Hossain and Takhar [19] studied the effect of thermal radiation using the Rosseland diffusion approximation on mixed convection together with a vertical plate with surface temperature and uniform free stream velocity. Furthermore, numerical solution for the collective consequences of thermal radiation and convective surface heat transfer on the laminar physical phenomenon in a few flat plate in a very uniform stream of fluid and a few moving plate in an exceedingly quiescent ambient fluid has been studied by Bataller [20]. Moreover, Olanrewaju et al. [21] studied convective surface condition for the radiation and viscous dissipation influences for the Blasius and Sakiadis flows. Aziz [22, 23] investigated a similarity solution for the laminar thermal boundary layer over a flat plate with a convective surface boundary condition and studied hydrodynamic with thermal slip boundary layer flow over a flat plate with a constant heat flux boundary condition. Garg et al. [24] studied a similarity solution for the laminar thermal boundary layer over a flat plate with internal heat generation and a convective surface boundary condition.

However, to the best of authors' knowledge, no analytical study has been previously reported on the analysis of effect of thermal radiation, buoyancy, and internal heat generation on flow and heat transfer in the Blasius flow over a plate with convective surface boundary conditions. In consideration of this and its significance in various technological applications, engineering, and numerous production processes, the authors of the present paper aim to examine the effect of various relevant parameters in the flow model like thermal radiation, the Prandtl number, internal heat generation, the Grashof number, and the Biot number on flow and heat transfer in the Blasius flow by the use of the optimal homotopy asymptotic method (OHAM). The effectiveness, generalization, and reliability of the proposed method have been proved in many research papers and several authors [25–29] who obtained solutions of currently important applications in science and engineering by using this method. In OHAM, the control and adjustment of the convergence region are provided in an expedient way. Moreover, OHAM is parameter-free and provides better accuracy over the approximate analytical methods at the identical order of approximation.

2. Basic Principles of the Optimal Homotopy Asymptotic Method (OHAM)

We review the fundamental principles of OHAM as expanded by Marinca et al. [30] and other researchers. Consider the subsequent differential equation:

$$L(z(x)) + r(x) + N(z(x)) = 0, x \in \Omega, \tag{1}$$

with boundary condition:

$$B\left(x, \frac{dz}{dx}\right) = 0, \tag{2}$$

where Ω is problem domain, L and N are linear and nonlinear operators, $z(x)$ is an unknown function, and $r(x)$ could

be a known function. An optimal homotopy equation (also called deformation equation) is made as

$$(1-p)[L(\phi(x;p)+a(x)] = h(p)[L(\phi(x;p))+a(x)+N(\phi(x;p))+a(x)], \quad (3)$$

where $0 \le p \le 1$ is an embedding parameter.

$h(p) = \sum_{k=1}^{m} p^k c_k$ is an auxiliary function on which the convergence of the answer relies. The auxiliary function $h(p)$ helps to regulate the convergence domain moreover on control the convergence region. If the function $\phi(x;p,c_j)$ is expanded in Taylor's series about p, the subsequent approximate solution is obtained:

$$\phi(x;p,c_j) = z_0(x) + \sum_{k=1}^{\infty} z_k(x,c_j)p^k, j = 1,2,3\cdots. \quad (4)$$

It has been observed by many researchers that the convergence of the series Eq. (4) depends upon the values of $c_{j,}(j = 1,2,3,\cdots m)$. Hence, if it is convergent, then

$$\tilde{z} = z_0(x) + \sum_{k=1}^{m} z_k(x;c_j). \quad (5)$$

Using Eq. (5) in Eq. (1) leads to the subsequent residual:

$$R(x;c_j) = L\left(\tilde{z}(x;c_j)\right) + r(x) + N\left(\tilde{z}(x;c_j)\right). \quad (6)$$

If $R(x;c_j) = 0$, then $z^{\sim}$ is the precise solution, but this is not the case usually in nonlinear problems. The values of $c_{j,}(j = 1,2,3,\cdots m)$ will be optimally identified via various methods like colocation method, methods of least square, Galerkin's method, the Ritz method, and the Kantorovich method which are often utilized. Finally, substituting these convergence control parameters in Eq. (5), one can get the approximate solution of the matter. During this study, we used the tactic of least square to search out the optimal values of the convergence control parameters.

3. Mathematical Formation

Consider a two-dimensional steady incompressible fluid flow with heat transfer by convection over a vertical plate. A stream of cold fluid at temperature T_∞ moved over the right surface of the plate with unvarying velocity U_∞ whilst the left surface of the plate was heated by convection from a hot fluid at temperature T_f which provided a heat transfer coefficient h_f. The density variation as a result of buoyancy force effects was taken under consideration with the momentum equation, and also, the thermal radiation and the inner heat generation effects were taken into account within the energy equation. Thus, the equations describing the flow are as follows [22, 31]:

Continuity equation:

$$\frac{\partial u}{\partial x} + \frac{\partial v}{\partial y} = 0. \quad (7)$$

Momentum equation:

$$u\frac{\partial u}{\partial x} + v\frac{\partial u}{\partial y} = \upsilon\frac{\partial^2 u}{\partial y^2} + g\beta(T - T_\infty) - \frac{\delta}{\rho}B_0^2 u. \quad (8)$$

Energy equation:

$$u\frac{\partial T}{\partial x} + v\frac{\partial T}{\partial y} = \frac{k}{\rho c_p}\frac{\partial^2 T}{\partial y^2} - \frac{1}{\rho c_p}\frac{\partial q_r}{\partial y} + \frac{Q_o}{\rho c_p}(T - T_\infty), \quad (9)$$

where u and v are the speed components along the flow direction (x-direction) and normal to flow direction (y-direction), υ is the kinematic viscosity, k is the thermal conductivity, δ is the electrical conductivity of the base fluid, c_p is that the specific heat of the fluid at constant pressure, ρ is the density, q_r is the radiative heat flux in the y-direction, Q_o is the heat released per unit mass, T is the temperature of the fluid inside the thermal physical phenomenon, g is the gravitational acceleration, β is the thermal volumetric expansion coefficient, B_0 is imposed flux, and T_∞ is the constant temperature of the ambient fluid. It is assumed that the viscous dissipation is neglected, the physical properties of the fluid are constant, and therefore, the Boussinesq and boundary layer approximation is also adopted for steady streamline flow. The fluid is taken into account to be gray, absorbing-emitting radiation but nonscatter medium.

The velocity boundary conditions at the plate and far-off from the plate are

$$u(x,0) = v(x,0) = 0, u(x,\infty) \longrightarrow u_\infty. \quad (10)$$

The thermal boundary conditions are expressed as

$$-k\frac{\partial T}{\partial y}(x,0) = h_f\left[T_f - T(x,0)\right], T(x,\infty) = T_\infty, \quad (11)$$

where u_∞ is a constant free stream velocity and h_f is the heat transfer coefficient. The radiative heat flux q_r is described by the Rosseland approximation such that

$$q_r = -\frac{4\sigma^*}{3k'}\frac{\partial T^4}{\partial y}, \quad (12)$$

where k' and σ^* are the mean absorption coefficient and the Stefan-Boltzmann constant, respectively. We undertake that the temperature alterations inside the flow are very small, so that T^4 can be expressed as linear function once the Taylor series was used to expand T^4 about the streamline temperature T_∞, and neglecting higher order terms results the subsequent approximation:

$$T^4 \cong 4T_\infty^3 T - 3T_\infty^4. \quad (13)$$

By using Eqs. (12) and (13), we obtain

$$q_r = \frac{-16\sigma^* T_\infty^3}{3k'}\frac{\partial T}{\partial y}. \quad (14)$$

Plugging Eq. (14) in to Eq. (9), we get

$$u\frac{\partial T}{\partial x}+v\frac{\partial T}{\partial y}=\left(\alpha+\frac{16\sigma^{*}T_{\infty}^{3}}{3k'}\cdot\frac{\alpha}{k}\right)\frac{\partial^{2}T}{\partial y^{2}}+\frac{\alpha}{k}Q_{o}(T-T_{\infty}), \tag{15}$$

where $\alpha = k/\rho c_p$ is the thermal diffusivity.

If we take $Ra = kk'/(4\sigma^{*}T_{\infty}^{3})$ as the radiation parameter in Eq. (15), we get

$$u\frac{\partial T}{\partial x}+v\frac{\partial T}{\partial y}=\frac{\alpha}{k_{o}}\cdot\frac{\partial^{2}T}{\partial y^{2}}+\frac{\alpha}{k}Q_{o}(T-T_{\infty}), \tag{16}$$

where $k_o = 3Ra/(3Ra+4)$.

To achieve the similarity solution of the problem, we define similarity variable η and stream function $f(\eta)$, and the nondimensional form of the temperature $\theta(\eta)$ is

$$\eta=y\sqrt{\frac{u_{\infty}}{\upsilon x}},\ \frac{u}{u_{\infty}}=f',\ v=\frac{1}{2}\sqrt{\frac{u_{\infty}\upsilon}{x}}\left(\eta f'-f\right),\ \theta(\eta)=\frac{T-T_{\infty}}{T_{w}-T_{\infty}}, \tag{17}$$

where $f' = df/d\eta$, u_∞ is an unceasing free stream velocity, and T_w is a constant temperature of the wall. From Eq. (17), we obtain

$$\frac{\partial u}{\partial x}=-\frac{u_{\infty}f''\eta}{2x},\ \frac{\partial v}{\partial y}=\frac{u_{\infty}\eta f''}{2x},\ \frac{\partial^{2}u}{\partial y^{2}}=\frac{u_{\infty}^{2}}{\upsilon x}f'''. \tag{18}$$

Equations (7) and (18) demonstrate the equation of continuity that holds.

Using Eqs. (8), (17), and (18), we obtain

$$f'''+\frac{1}{2}ff''+Gr_{x}\theta-Mf'=0, \tag{19}$$

where

$$Gr_{x}=\frac{g\beta(Tw-T_{\infty})x}{u_{\infty}^{2}}\ \text{and}\ M=\frac{\delta B_{0}^{2}x}{\rho u_{\infty}}, \tag{20}$$

in which Gr_x and M, respectively, represent the local Grashof number and the magnetic field parameter.

From Eq. (17), we can also obtain

$$\frac{\partial T}{\partial x}=\frac{-\theta'\eta}{2x}(T_{w}-T_{\infty}),\ \frac{\partial T}{\partial y}=\theta'\sqrt{\frac{u_{\infty}}{\upsilon x}}(T_{w}-T_{\infty}),\ \frac{\partial^{2}T}{\partial y^{2}}=\theta''\frac{u_{\infty}}{\upsilon x}(T_{w}-T_{\infty}). \tag{21}$$

Substituting Eqs. (17), (18), and (21) in to Eq. (16), we get

$$\theta''+k_{o}\ \mathrm{Pr}\left(\frac{1}{2}f\theta'+\lambda\theta\right)=0, \tag{22}$$

where $\mathrm{Pr} = \upsilon/\alpha$ is the Prandtl number and $\lambda_x = Q_o x/(u_\infty \rho c_p)$ is the internal heat generation.

Using Eqs. (10), (11), and (17), we get the transformed boundary conditions, and they are as follows:

$$\left.\begin{aligned} &f(0)=f'(0)=0, \quad \theta'(0)=-Bi[1-\theta(0)],\\ &f'(\infty)=1, \qquad\quad \theta(\infty)=0. \end{aligned}\right\} \tag{23}$$

For the momentum and energy equations to have a similarity solution, the parameters Gr, λ, and M must be constants, not functioning as variable x as expressed above [20, 32]. This circumstance can be met if the imposed magnetic field B_0 is proportional to $x^{-1/2}$ and the heat released/unit mass Q_o, and the thermal expansion coefficient β is proportional to x^{-1}. We therefore take

$$\begin{aligned} B_{0}&=cx^{\frac{-1}{2}},\\ \beta&=mx^{-1},\\ Q_{0}&=sx^{-1}, \end{aligned} \tag{24}$$

where c, m, and s are constants. With these assumptions, we have

$$\begin{aligned} Gr&=\frac{mg\upsilon(T_{w}-T_{\infty})}{u_{\infty}^{2}},\\ M&=\frac{c^{2}\delta}{\rho u_{\infty}},\\ \lambda&=\frac{s}{u_{\infty}\rho c_{p}}. \end{aligned} \tag{25}$$

4. Solution of the Problem by the Proposed Method

Applying OHAM on the nonlinear ordinary differential Eqs. (19) and (22), we develop a family of equations:

$$\left.\begin{aligned} &(1-p)\left(f'''\right)-h_{1}(p)\left[f'''+\frac{1}{2}ff''+Gr\theta-Mf'\right]=0\\ &(1-p)\left(\theta''\right)-h_{2}(p)\left[\theta''+k_{o}\ \mathrm{Pr}\left(\frac{1}{2}f\theta'+\lambda\theta\right)\right]=0, \end{aligned}\right\} \tag{26}$$

where $p \in [0, 1]$ and the primes indicate differentiation of the function f with respect to η.

We consider $f, \theta, h_1(p)$, and $h_2(p)$ as follows:

$$\begin{aligned} &f=f_{0}+pf_{1}+p^{2}f_{2}+p^{3}f_{3}, \quad \theta=\theta_{0}+p\theta_{1}+p^{2}\theta_{2}+p^{3}\theta_{3},\\ &h_{1}(p)=pc_{1}+p^{2}c_{2}+p^{3}c_{3}, \quad h_{2}(p)=pc_{4}+p^{2}c_{5}+p^{3}c_{6}. \end{aligned} \tag{27}$$

Plugging Eq. (27) into Eq. (26) and simplifying, rearranging, and collecting terms with common powers of p, we obtain the following zero-, first-, second-, and third-order problems with regard to their boundary conditions.

Zero-order problems:

$$f_0'(\eta) = 0, \theta_0'(\eta) = 0. \tag{28}$$

Subject to the boundary conditions:

$$\left.\begin{aligned} f_0(0) = f_0{}'(0) = 0, \quad & f_0{}'(\infty) = 1, \\ \theta_0{}'(0) = -Bi(1-\theta(0)), \quad & \theta_0(\infty) = 0. \end{aligned}\right\} \tag{29}$$

And its solution is

$$\left.\begin{aligned} f_0(\eta) &= \frac{1}{2n}\eta^2 \\ \theta_0(\eta) &= Bi(1-\theta(0))(n-\eta). \end{aligned}\right\} \tag{30}$$

The first-order problems:

$$\left.\begin{aligned} f_1'(\eta, c_1) &= c_1\left(\frac{1}{2}f_0 f_0' + Gr_x\theta_0 - Mf_0'\right) \\ \theta_1'(\eta, c_1) &= c_4 pr\left(\frac{1}{2}k_0 f_0\theta_0' + \lambda k_0\theta_0\right), \end{aligned}\right\} \tag{31}$$

with boundary conditions:

$$\left.\begin{aligned} f_1(0) = f_1{}'(0) = f_1{}'(\infty) = 0, \\ \theta_1{}'(0) = \theta_1(\infty) = 0. \end{aligned}\right\} \tag{32}$$

Its solution is

$$\left.\begin{aligned} f_1(\eta, c_1) &= c_1\left[\frac{1}{48}\left(\frac{\eta^5}{5n^2} - \frac{n\eta^2}{2}\right) + \frac{Gr_x n}{6}a(1-\theta(0))\left(\eta^3 - \frac{\eta^4}{4n} - n\eta^2\right) - \frac{M}{12}\left(\frac{\eta^4}{2n} - n\eta^2\right)\right] \\ \theta_1(\eta, c_4) &= c_4 prn^3 a(1-\theta(0))\left(\frac{-k_0}{48}\left(\frac{\eta^4}{n^4} - 1\right) + k_0\lambda\left(\frac{\eta^2}{2n^2} - \frac{\eta^3}{6n^3} - \frac{1}{3}\right)\right). \end{aligned}\right\} \tag{33}$$

The second-order problems:

$$\left.\begin{aligned} f_2'(\eta, c_1, c_2) &= (1+c_1)f_1' + c_1\left(\frac{1}{2}f_0 f_1' + \frac{1}{2}f_1 f_0' + Gr_x\theta_1 - Mf_1'\right) + c_2\left(\frac{1}{2}f_0 f_0' + Gr_x\theta_0 - Mf_0'\right) \\ \theta_2'(\eta, c_4, c_5) &= (1+c_4)\theta_1' + \frac{1}{2}k_0 pr\left[\left(c_4\theta_1' + c_5\theta_0'\right)f_0 + c_4\theta_0' f_1\right] + pr\lambda k_0(c_4\theta_1 + c_5\theta_0). \end{aligned}\right\} \tag{34}$$

Subject to the boundary conditions:

$$\left.\begin{aligned} f_2(0) = f_2'(0) = f_2'(\infty), \\ \theta_2'(0) = 0, \theta_2(\infty) = 0. \end{aligned}\right\} \tag{35}$$

Its solution is

$$\begin{aligned} f_2(\eta, c_1, c_2) = {} & (1+c_1)c_1\left[\frac{1}{48}\left(\frac{\eta^5}{5n^2} - \frac{n\eta^2}{2}\right) + Gr_x nBi(1-\theta(0))\left(\frac{\eta^3}{6} - \frac{\eta^4}{24n} - \frac{n\eta^2}{6}\right) - \frac{M}{12}\left(\frac{\eta^4}{2n} - n\eta^2\right)\right] \\ & + c_1\left(\begin{array}{c} \frac{c_1}{24}\left(\frac{1}{8}\left(\frac{\eta^8}{84n^3} - \frac{\eta^5}{60} - \frac{n^3\eta^2}{168}\right) + Gr_x Bi(1-\theta(0))\left(\frac{\eta^6}{20} - \frac{\eta^7}{70n} - \frac{n\eta^5}{30} - \frac{n^4\eta^2}{60}\right) - M\left(\frac{\eta^7}{70n^2} - \frac{\eta^5}{60} - \frac{n^3\eta^2}{120}\right)\right) \\ + \frac{1}{12}c_1\left(\frac{1}{8}\left(\frac{\eta^8}{1680n^3} - \frac{\eta^5}{120} + \frac{31n^3\eta^2}{1680}\right) + Gr_x Bi(1-\theta(0))\left(\frac{\eta^6}{120} - \frac{\eta^7}{840n} - \frac{n\eta^5}{60} + \frac{n^4\eta^2}{48}\right) - \frac{M}{2}\left(\frac{\eta^7}{420n^2} - \frac{\eta^5}{60} + \frac{n^3\eta^2}{30}\right)\right) \\ + Gr_x c_4 prBi(1-\theta(0))\left[\frac{k_0}{48}\left(\frac{n^3\eta^3}{6} - \frac{\eta^7}{210n} - \frac{7n^4\eta^2}{30}\right) + \lambda\left(\frac{n\eta^5}{120} - \frac{\eta^6}{720} - \frac{n^3\eta^3}{18} + \frac{n^4\eta^2}{15}\right)\right] \\ \frac{-Mc_1}{6}\left(\frac{1}{8}\left(\frac{\eta^7}{210n^2} - \frac{n\eta^4}{24} + \frac{n^3\eta^2}{15}\right) + Gr_x Bi(1-\theta(0))\left(\frac{n\eta^5}{20} - \frac{\eta^6}{120} - \frac{n^2\eta^4}{12} + \frac{n^4\eta^2}{15}\right) - M\left(\frac{\eta^6}{120n} - \frac{n\eta^4}{24} + \frac{7n^3\eta^2}{120}\right)\right) \end{array}\right) \\ & + c_2\left(\frac{1}{48}\left(\frac{\eta^5}{5n^2} - \frac{n\eta^2}{2}\right) + Gr_x nBi(1-\theta(0))\left(\frac{\eta^3}{6} - \frac{\eta^4}{24n} - \frac{n\eta^2}{6}\right) - \frac{M}{6}\left(\frac{\eta^4}{4n} - \frac{n\eta^2}{2}\right)\right). \end{aligned}$$

$$\theta_2(\eta, c_4, c_5) = prn^3 Bi(1-\theta(0))\left[\begin{array}{c} (1+c_4)c_4\left[\frac{k_0}{48}\left(1 - \frac{\eta^4}{n^4}\right) + \lambda\left(\frac{\eta^2}{2n^2} - \frac{\eta^3}{6n^3} - \frac{1}{3}\right)\right] \\ +\frac{1}{4}k_0\left(\begin{array}{c} {c_4}^2 prn^2\left(\frac{k_0}{504}\left(1 - \frac{\eta^7}{n^7}\right) + \lambda\left(\frac{\eta^5}{20n^5} - \frac{\eta^6}{60n^6} - \frac{1}{30}\right)\right) - \frac{c_5}{12}\left(1 - \frac{\eta^4}{n^4}\right) \\ -c_1 c_4 n^2\left[\begin{array}{c} \frac{1}{24}\left(\frac{\eta^7}{210n^7} - \frac{\eta^4}{24n^4} + \frac{31}{840}\right) \\ +\frac{Gr_x na(1-\theta(0))}{3}\left(\frac{\eta^5}{20n^5} - \frac{\eta^6}{120n^6} - \frac{\eta^4}{12n^4} + \frac{5}{120}\right) - \frac{M}{6}\left(\frac{\eta^6}{60n^6} - \frac{\eta^4}{12n^4} + \frac{1}{15}\right) \end{array}\right] \end{array}\right) \\ +\lambda\left[c_5\left(\frac{\eta^2}{2n^2} - \frac{\eta^3}{6n^3} - \frac{1}{3}\right) + {c_4}^2 prn^2\left(\frac{k_0}{48}\left(\frac{\eta^2}{2n^2} - \frac{\eta^6}{30n^6} - \frac{7}{15}\right) + \lambda\left(\frac{\eta^4}{24n^4} - \frac{\eta^5}{120n^5} - \frac{\eta^2}{6n^2} + \frac{2}{15}\right)\right)\right] \end{array}\right]. \tag{36}$$

Third-order problems:

$$\left.\begin{aligned} f_3'(\eta, c_1, c_2, c_3) &= (1+c_1)f_2'' + c_2 f_1'' + \frac{1}{2}c_1\left(f_1 f_1' + f_0 f_2' + f_0'' f_2\right) + \frac{1}{2}c_2\left(f_0 f_1' + f_0' f_1\right) + \frac{1}{2}c_3 f_0 f_0' + Gr_x(c_1\theta_2 + c_2\theta_1 + c_3\theta_0) + c_3 f_0'' - M\left(c_1 f_2' + c_2 f_1' + c_3 f_0'\right) \\ \theta_3'(\eta, c_4, c_5, c_6) &= (1+c_4)\theta_2' + c_5\theta_1' + \frac{1}{2}Prk_0\left[\left(c_4\theta_2' + c_5\theta_1' + c_6\theta_0'\right)f_0 + \left(c_4\theta_1' + c_5\theta_0'\right)f_1 + c_4\theta_0' f_2\right] + Pr\lambda k_0(c_4\theta_2 + c_5\theta_1 + c_6\theta_0). \end{aligned}\right\} \tag{37}$$

Subject to boundary conditions:

$$\left.\begin{aligned} f_3(0) = f_3'(0) = f_3'(\infty), \\ \theta_3'(0) = \theta_3(\infty) = 0. \end{aligned}\right\} \tag{38}$$

Also, the solution for Eq. (37) subject to Eq. (38) is found in the same way, but they are too large expressions to be included in this paper. Adding up the solution components the four-term solution obtained by OHAM, for $p = 1$, is

$$\left\{\begin{aligned} \tilde{f}(\eta, c_1, c_2) &= f_0(\eta) + f_1(\eta, c_1) + f_2(\eta, c_1, c_2) + f_3(\eta, c_1, c_2, c_3) \\ \tilde{\theta}(\eta, c_4, c_5) &= \theta_0(\eta) + \theta_1(\eta, c_4) + \theta_2(\eta, c_4, c_5) + \theta_3(\eta, c_4, c_5, c_6). \end{aligned}\right. \tag{39}$$

In order to determine the values of convergence control parameters in Eq. (36), we used the least square method for $\mathrm{Pr} = 0.72, \mathrm{Gr} = \mathrm{Ra} = \mathrm{M} = \lambda = 0.1$, and we get $c_1 = 0.031077$; $c_2 = -0.134380$; $c_3 = -0.006856$; $c_4 = -0.074109$; $c_5 = 0.003043$; $c_6 = 2.236272$..

5. Result and Discussion

The governing PDEs are converted into a system of nonlinear ODEs (Eqs. (19) and (22)) with boundary conditions (Eq. (23)) by a suitable similarity transformation technique, and these transformed equations are solved systematically by the use of optimal homotopy asymptotic method. Analytical approximate solutions for the velocity and fluid temperature have been obtained for diverse embedded parameters in the flow model controlling the liquid flow within the flow framework. The impact of various relevant parameters in the governing equations of the flow model on the velocity and temperature of the liquid has been displayed for different values of the Prandtl number *Pr*, internal heat generation λ, the Biot number *Bi*, radiation parameter *Ra*, and the Grashof number *Gr*. The outcomes have been compared with the result of other researchers for limited case and displayed in tables and figures for specific parameters.

5.1. Comparative Analysis. To confirm the accuracy and appropriateness of the method, we have compared the value of the skin-friction coefficient $f''(0)$ and the *temperature gradient* at the wall $-\theta'(0)$ obtained by the present method with the results reported by previous studies under limiting conditions [13, 21, 22, and 22]. The comparison of the obtained result is presented in Tables 1 and 2, which illustrates an excellent agreement. Hence, we are confident that the method is suitable for examination of the problem. Table 1 displays the comparison of values of the nearby Nusselt number $-\theta'(0)$ and the skin-friction coefficient $f''(0)$ obtained by utilizing the OHAM with the numerical result reported by Olanrewaju et al. [21] for diverse values of inserted parameters within the flow model, and it shows an excellent agreement. It is evident from the table that the rate of heat exchange at the plate surface $-\theta'(0)$ and the skin-friction coefficient $f''(0)$ intensifies with increasing values of the Grashof number *Gr*, internal heat generation parameter λ, convective heat transfer parameter *Bi*, and thermal radiation parameter *Ra*. However, an increment in the fluid Prandtl number diminishes the skin-friction but upsurges the rate of heat transfer at the plate surface. In Table 2, comparison of the results of the Nusselt number and surface temperature of the fluid for different value of Biot number with the previously reported data in the cited literature is presented. As it is observed in Table 2, the results are in good agreement with the results reported by Solomon and Mitiku [13], Olanrewaju et al. [21], and Aziz [22]. From the table, it is also obvious that both the Nusselt number and surface temperature rise with the Biot number.

In Figures 1–5, the effects of various parameters on the nondimensional velocity profiles inside the boundary layer have been displayed. For the most part, the fluid speed is zero at the plate surface and expanded gradually away from the plate towards the free stream value satisfying the boundary condition. Figures 1–3 show that an increase in the value of the Prandtl number, thermal radiation, and internal heat generation parameter has an immaterial impact on the fluid velocity even if the velocity profile shows a bit decreasing trend as the esteem of *Pr* increased and shows a little increasing tendency as the values of thermal radiation and internal heat generation parameters increased. Actually, fluid viscosity has a tendency to increase with increasing resistance to distortion which leads to a reduction within the velocity profile as the Prandtl number increases, but it has a trend to decrease as internal heat generation and thermal radiation increase.

The impact of the Grashof number on the velocity profiles is exhibited in Figure 4. It is seen from the figure that an increment within the buoyancy force causes to increase in the velocity profile. Physically, an increase in *Gr* adds more thermal energy into the fluid molecules and loosens up intermolecular forces within the fluid particles which means the

Table 1: Comparison of value of the skin-friction coefficient and the Nusselt number obtained by OHAM with numerical solutions reported by other researchers for various parameters.

Pr	Gr	Bi	λ	Ra	By Olanrewaju et al. [21]		Present result	
					$f''(0)$	$-\theta'(0)$	$f''(0)$	$-\theta'(0)$
0.72	0.1	0.1	0.1	0.1	0.386316	0.066810	0.386325	0.066809
0.72	0.1	1	0.1	0.1	0.460825	0.176790	0.460827	0.176789
0.72	0.1	10	0.1	0.1	0.483261	0.213880	0.483259	0.213878
0.72	0.5	0.1	0.1	0.1	0.557241	0.069730	0.557250	0.069732
0.72	1	0.1	0.1	0.1	0.723310	0.071736	0.723308	0.071737
0.72	0.1	0.1	0.5	0.1	0.280070	0.110631	0.280069	0.110629
0.72	0.1	0.1	0.6	0.1	0.298365	0.102052	0.298367	0.102048
0.72	0.1	0.1	0.1	0.5	0.392337	0.065305	0.392336	0.065312
0.72	0.1	0.1	0.1	1	0.398724	0.063698	0.398719	0.0636987
0.72	0.1	0.1	0.1	2	0.408879	0.061177	0.408881	0.061169
3.00	0.1	0.1	0.1	0.1	-0.074540	0.231312	-0.074538	0.231315
7.10	0.1	0.1	0.1	0.1	-0.015860	0.261733	-0.015858	0.261729

Table 2: Comparison of the results of the Nusselt number and surface temperature for different values of Bi with results reported by Solomon and Mitiku [13], Olanrewaju et al. [21], and Aziz [22].

Bi	Present result		Solomon and Mitiku [13]		Olanrewaju et al. [21]		Aziz [22]	
	$-\theta'(0)$	$\theta(0)$	$-\theta'(0)$	$\theta(0)$	$-\theta'(0)$	$\theta(0)$	$-\theta'(0)$	$\theta(0)$
0.05	0.0427638	0.144652	0.042764	0.14464	0.042767	0.14466	0.0428	0.1447
0.10	0.0747231	0.252749	0.074722	0.25272	0.074724	0.25275	0.0747	0.2528
0.20	0.11929589	0.403534	0.119296	0.40351	0.119295	0.40352	0.1193	0.4035
0.40	0.1699937	0.575009	0.169993	0.57501	0.169994	0.57501	0.1700	0.5750
0.60	0.1980488	0.669908	0.198049	0.66990	0.198051	0.66991	0.1981	0.6699
0.80	0.2158631	0.730177	0.215862	0.73015	0.215864	0.73016	0.2159	0.7302
1.00	0.2281776	0.771786	0.228176	0.77179	0.228178	0.77181	0.2282	0.7718
5.00	0.2791322	0.944155	0.279129	0.94415	0.279131	0.94417	0.2791	0.9441
10.00	0.2871457	0.971278	0.287145	0.97127	0.287146	0.97128	0.2871	0.9713
20.00	0.2913293	0.985429	0.291331	0.98541	0.291329	0.98543	0.2913	0.9854
30.00	0.2927542	0.990237	0.292752	0.99023	0.292754	0.99024	—	—

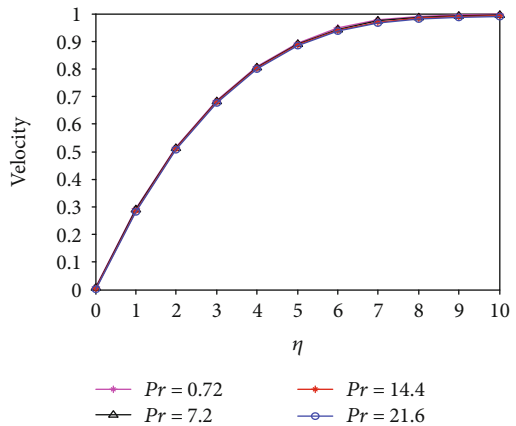

Figure 1: Velocity profiles for varied values of Pr once $Gr = \lambda = M = Bi = Ra = 0.1$.

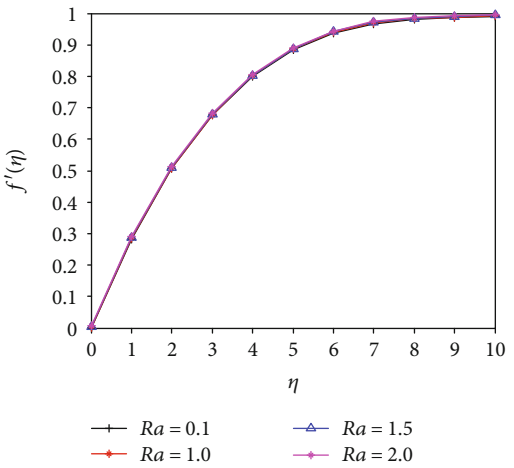

Figure 2: Velocity profiles for unlike values of Ra once $Pr = 0.72$, $Gr = 0.1$, $M = 0.1$, $\lambda = 0.1$, and $Bi = 0.1$.

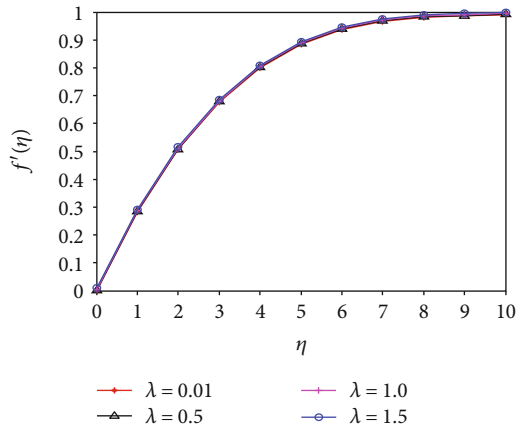

Figure 3: Velocity profiles for altered values of λ once $Pr = 0.72$, $Gr = M = Bi = Ra = 0.1$.

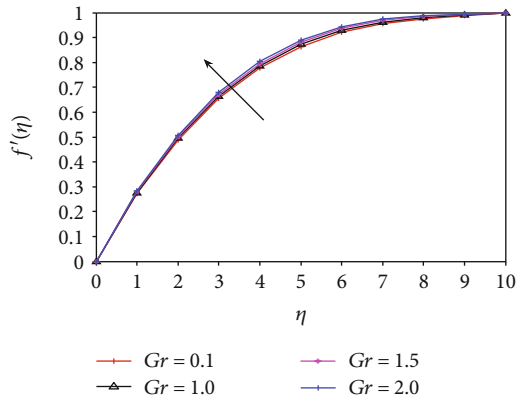

Figure 4: Velocity profiles for altered values of Gr once $Pr = 0.72$, $\lambda = M = Bi = Ra = 0.1$.

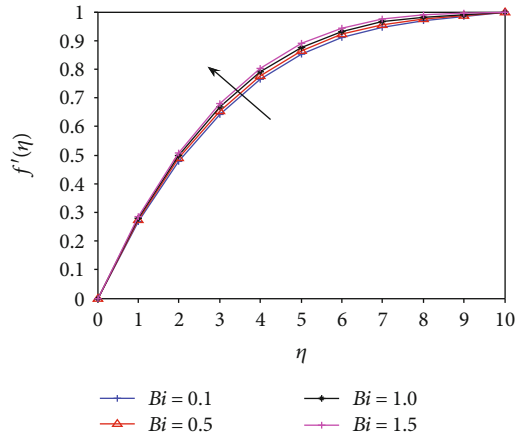

Figure 5: Velocity profiles for altered values of Bi once $Pr = 0.72$, $Gr = \lambda = M = Ra = Bi = 0.1$.

fluid is less viscous due to an increase in temperature. Thus, the force resists the motion, viscous force reduces, and buoyancy drive acts as a pressure gradient to advance the stream. Hence, the velocity of the fluid and local heat transfer boosts with increasing in the value of Gr because Gr is the ratio of the buoyant to viscous force acting on a fluid in the velocity

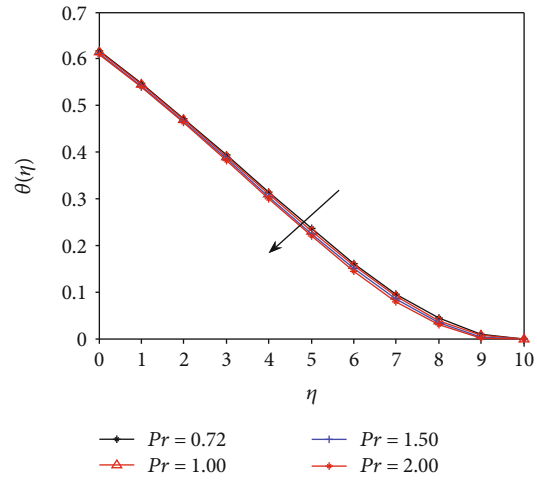

Figure 6: Temperature profiles for sundry values of Pr once $\lambda = M = Gr = Ra = Bi = 0.1$.

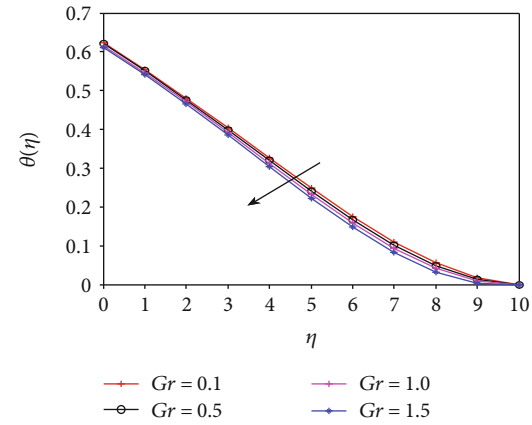

Figure 7: Temperature profiles for sundry values of Gr once $Pr = 0.72$, $\lambda = M = Ra = Bi = 0.1$.

boundary layer. In Figure 5, the impact of the Biot number on the fluid velocity profile is revealed. It is observed that the fluid velocity increased with the Biot number. This happens because the plate surface is convectively heated and the flow gets to be speedier. In reality, when fluids are heated their density reduces and buoyancy increases. The increment in bouncy force is responsible to the momentum boundary layer thickness become elongated and results in the boosting of the fluid velocity.

In Figures 6–10, the effects of various physical parameters in the flow model on the fluid temperature inside the boundary layer are displayed. The figures illustrated that the fluid temperature is a peak at the plate surface and exponentially reduced to zero at a distance far away from the plate satisfying boundary conditions. From Figure 6, we noticed that snowballing in the values of the Prandtl number leads to dropping the fluid temperature profile and the thermal boundary layer thickness. The reason behind this phenomenon is that thermal diffusivity decreases against the Prandtl number as they have inverse relation and leads to a lessening in the fluid temperature. Physically, an increment in the

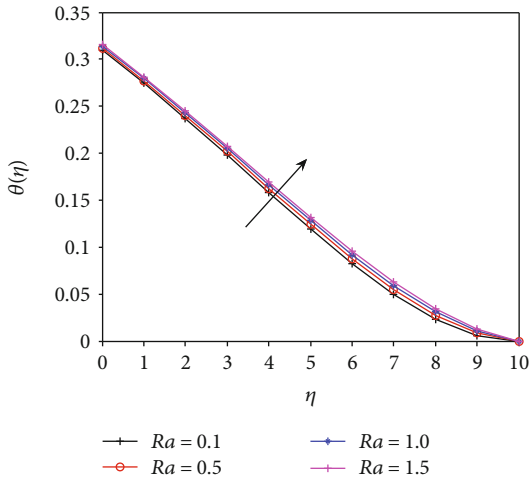

Figure 8: Temperature profiles for sundry values of Ra once $Pr = 0.72$, $\lambda = M = Bi = Gr = 0.1$.

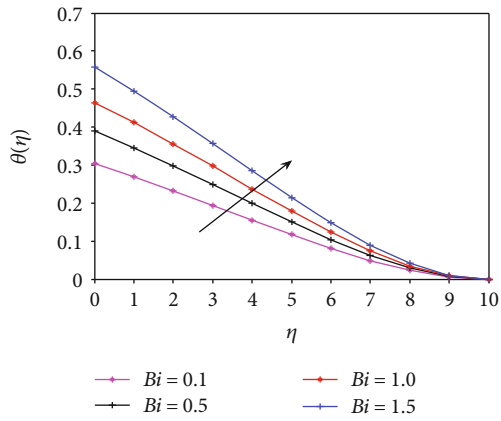

Figure 9: Temperature profiles for various values of Bi once $Pr = 0.72$, $\lambda = M = Gr = Ra = 0.1$.

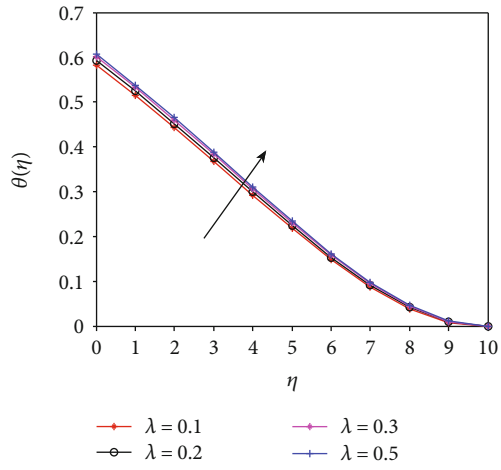

Figure 10: Temperature profiles for various values λ once $Pr = 0.72$, $Gr = 0.72$, $M = Bi = Ra = 0.1$.

Prandtl number implies an increase in fluid viscosity which in turn causes a reduction in the temperature distribution. The effect of the Grashof number on the temperature profile is presented in Figure 7. It is observed that raising the values of the Grashof number diminishes the fluid temperature profile. This happens because when Gr increases, the fluid particle gathers more momentum which causes additional heat flow to the surrounding and thereby reduces the temperature profile.

In Figure 8, we found out that the temperature profile increased with the increased values of Ra which shows that the thermal boundary layer thickness enlarges with the increase in the thermal radiation. Physically, radiation is considered a process of energy transfer which extracts energy by moving particles, which upsurges the thermal conductivity of moving liquid. Therefore, higher radiation parameter results in a greater heat production in the flow which in turn leads to an increase in temperature profile of the fluid. As illustrated in Figure 9, the fluid temperature increases with snowballing the values of the Biot number, and the thermal boundary layer becomes thicker due to the convective heat transfer from the warm fluid on the left surface of the plate to the freezing fluid on the right surface. This then causes the fluid to heat up so increasing the fluid temperature deliveries. From the mathematical point of view, increasing the values of the Biot number means the convective heat transfer extent increases, thereby enhancing additional heat transfer from the surface which results in temperature distribution of the flow to rise. From Figure 10, we have seen that the temperature profile increases with internal heat generation. This illustrates the presence of an exponentially decaying internal heat generation within the flow system brings to reinforce the thermal boundary layer thickness.

6. Conclusion

In this work, a two-dimensional steady incompressible fluid flow with heat transfer by convection over a vertical plate is considered. A stream of cold fluid at temperature T_∞ moved over the right surface of the plate with constant velocity U_∞ whilst the left surface of the plate was heated by convection from a hot fluid at temperature T_f which provided a heat transfer coefficient h_f. The density variation as a result of buoyancy force effects was taken under consideration with the momentum equation, and also, the thermal radiation and the inner heat generation effects were taken into account within the energy equation. The nonlinear partial differential equation describing the flow problem is transformed into equivalent nonlinear ODEs using similarity variable transformation system and then solved analytically by the use of the OHAM. The impact of the combined effects of thermal radiation, internal heat generation, and buoyancy on temperature and velocity profile is analysed. To confirm the applicability and accuracy of the method, the obtained result is verified with some successful and available theoretical data in the literature. The comparative outcomes show an excellent agreement with the current computational analysis. We have taken into consideration the effects of radiation

parameter, internal heat generation, the Prandtl number Pr, Grashof number Gr, and Biot number Bi on speed and temperature profile of the fluid. From the result of the present study, the subsequent significant conclusions have been drawn:

(1) The temperature profile reduces with an increase in the value of the Prandtl number. Hence, higher Pr value causes a thinner thermal boundary layer. However, a significant impact is not determined on the fluid velocity with varying Pr even though it shows reduced tendency

(2) With an increase in the value of the Biot number, both the velocity and temperature profile of the fluid increase

(3) With the rise in value of the Grashof number, the fluid velocity increases; however, the fluid temperature profile diminishes

(4) The temperature profile of the fluid increases with increasing values of thermal radiation parameter, but significant effect is not ascertained in its velocity profile

(5) The temperature distribution of the fluid increase once the values of internal heat generation increases, but the variation in velocity profile is insignificant though slightly increasing tendency is ascertained. So, a higher value of internal heat generation causes thickening of the thermal boundary layer

(6) The skin-friction coefficient and the Nusselt number intensify with the Grashof number, internal heat generation, Biot number, and thermal radiation parameter

(7) With an increment in the Prandtl number, the skin-friction diminishes and the rate of heat transfer at the plate surface upsurges.

Nomenclature

T_∞: Constant temperature of the ambient fluid
T: Temperature of the fluid
T_w: Constant temperature of the wall
g: Gravitational acceleration
Gr: Grashof number
Pr: Prandtl number
q_r: Radiative heat flux
u_∞: Constant free stream velocity
u: Stream wise velocity
v: Normal velocity
k: Thermal conductivity
c_p: Specific heat at constant pressure
Q_o: Heat released per unit mass
B_0: Imposed flux
h_f: Heat transfer coefficient
υ: Kinematic viscosity
β: Thermal volumetric expansion coefficient
δ: Density of the fluid
σ^*: Stefan-Boltzmann constant
α: The thermal diffusivity
η: Similarity variable
θ: Nondimensional temperature
λ: Internal heat generation
x: Steamwise coordinate axis
y: Normal coordinate axis
k': Mean absorption coefficient
f: Stream function
M: Magnetic field parameter
Bi: Biot number
Ra: Thermal radiation parameter.

Data Availability

All the data used to support the findings of this study is included in the manuscript.

Conflicts of Interest

The authors declare that there is no conflict of interest regarding the publication of this work.

Acknowledgments

The authors would like to thank the Jimma University College of Natural sciences postgraduate program for the financial support they provided us.

References

[1] H. Blasius, "Boundary layers in fluids of small viscosity," *Zeitschrift für Angewandte Mathematik und Physik*, vol. 56, no. 1, pp. 1–37, 1908.

[2] T. Fang, "Similarity solutions for a moving-flat plate thermal boundary layer," *Acta Mechanica*, vol. 163, no. 3-4, pp. 161–172, 2003.

[3] O. D. Makinde, "Free convection flow with thermal radiation and mass transfer past a moving vertical porous plate," *International Communications in Heat and Mass Transfer*, vol. 32, no. 10, pp. 1411–1419, 2005.

[4] R. Cortell, "Flow and heat transfer of a fluid through a porous medium over a stretching surface with internal heat generation/absorption and suction/blowing," *Fluid Dynamics Research*, vol. 37, no. 4, p. 231, 2005.

[5] J.-J. Shu and P. Ioan, "On thermal boundary layers on a flat plate subjected to a variable heat flux," *International Journal of Heat and Fluid Flow*, vol. 19, no. 1, pp. 79–84, 1998.

[6] A. M. M. Abusitta, "A note on a certain boundary-layer equation," *Applied Mathematics and Computation*, vol. 64, no. 1, pp. 73–77, 1994.

[7] V. M. Falkneb and W. S. Sylvia, "LXXXV," *The London, Edinburgh, and Dublin Philosophical Magazine and Journal of Science*, vol. 12, no. 80, pp. 865–896, 1931.

[8] L. Wang, "A new algorithm for solving classical Blasius equation," *Applied Mathematics and Computation*, vol. 157, no. 1, pp. 1–9, 2004.

[9] M. G. Reddy, M. V. V. N. L. S. Rani, K. G. Kumar, B. C. Prasannakumar, and A. J. Chamkha, "Cattaneo–Christov heat flux

model on Blasius–Rayleigh–Stokes flow through a transitive magnetic field and Joule heating," *Physica A: Statistical Mechanics and its Applications*, vol. 548, article 123991, 2020.

[10] S. I. Abdelsalam and K. Vafai, "Combined effects of magnetic field and rheological properties on the peristaltic flow of a compressible fluid in a microfluidic channel," *European Journal of Mechanics-B/Fluids*, vol. 65, pp. 398–411, 2017.

[11] M. R. Krishnamurthy, B. C. Prasannakumara, R. S. R. Gorla, and B. J. Gireesha, "Non-linear thermal radiation and slip effect on boundary layer flow and heat transfer of suspended nanoparticles over a stretching sheet embedded in porous medium with convective boundary conditions," *Journal of Nanofluids*, vol. 5, no. 4, pp. 522–530, 2016.

[12] P.-Y. Xiong, A. Hamid, Y.-M. Chu et al., "Dynamics of multiple solutions of Darcy–Forchheimer saturated flow of Cross nanofluid by a vertical thin needle point," *The European Physical Journal Plus*, vol. 136, no. 3, pp. 1–22, 2021.

[13] S. B. Kejela and M. D. Firdi, "Analytical analysis of effects of buoyancy, internal heat generation, magnetic field, and thermal radiation on a boundary layer over a vertical plate with a convective surface boundary condition," *International Journal of Differential Equations*, vol. 2020, 16 pages, 2020.

[14] F. Mabood, A. K. Waqar, and I. M. I. Ahmad, "Analytical solution for radiation effects on heat transfer in Blasius flow," *International Journal of Modern Engineering Sciences*, vol. 2, no. 2, pp. 63–72, 2013.

[15] M. Gnaneswara Reddy, R. J. P. Gowda, R. N. Kumar, B. C. Prasannakumara, and K. G. Kumar, "Analysis of modified Fourier law and melting heat transfer in a flow involving carbon nanotubes," *Proceedings of the Institution of Mechanical Engineers, Part E: Journal of Process Mechanical Engineering*, vol. 2021, no. article 09544089211001353, 2021.

[16] B. Kuo, "Thermal boundary-layer problems in a semi-infinite flat plate by the differential transformation method," *Applied Mathematics and Computation*, vol. 150, no. 2, pp. 303–320, 2004.

[17] B. C. Sakiadis, "Boundary-layer behavior on continuous solid surfaces: I. Boundary-layer equations for two-dimensional and axisymmetric flow," *AICHE Journal*, vol. 7, no. 1, pp. 26–28, 1961.

[18] L. J. Crane, "Flow past a stretching plate," *Zeitschrift für angewandte Mathematik und Physik ZAMP*, vol. 21, no. 4, pp. 645–647, 1970.

[19] M. A. Hossain and H. S. Takhar, "Radiation effect on mixed convection along a vertical plate with uniform surface temperature," *Heat and Mass Transfer*, vol. 31, no. 4, pp. 243–248, 1996.

[20] R. Bataller, "Radiation effects for the Blasius and Sakiadis flows with a convective surface boundary condition," *Applied Mathematics and Computation*, vol. 206, no. 2, pp. 832–840, 2008.

[21] P. O. Olanrewaju, J. A. Gbadeyan, T. Hayat, and A. H. Awatif, "Effects of internal heat generation, thermal radiation and buoyancy force on a boundary layer over a vertical plate with a convective surface boundary condition," *South African Journal of Science*, vol. 107, no. 9-10, pp. 80–85, 2011.

[22] A. Aziz, "A similarity solution for laminar thermal boundary layer over a flat plate with a convective surface boundary condition," *Communications in Nonlinear Science and Numerical Simulation*, vol. 14, no. 4, pp. 1064–1068, 2009.

[23] A. Aziz, "Hydrodynamic and thermal slip flow boundary layers over a flat plate with constant heat flux boundary condition," *Communications in Nonlinear Science and Numerical Simulation*, vol. 15, no. 3, pp. 573–580, 2010.

[24] P. Garg, G. N. Purohit, and R. C. Chaudhary, "A similarity solution for laminar thermal boundary layer over a flat plate with internal heat generation and a convective surface boundary condition," *Journal of Rajasthan Academy of Physical Sciences*, vol. 14, no. 2, pp. 221–226, 2015.

[25] M. Esmaeilpour and D. G. Davood, "Solution of the Jeffery-Hamel flow problem by optimal homotopy asymptotic method," *Computers & Mathematics with Applications*, vol. 59, no. 11, pp. 3405–3411, 2010.

[26] A. Golbabai, F. Mojtaba, and S. Khosro, "Application of the optimal homotopy asymptotic method for solving a strongly nonlinear oscillatory system," *Mathematical and Computer Modelling*, vol. 58, no. 11-12, pp. 1837–1843, 2013.

[27] F. Mabood and A. K. Waqar, "Homotopy analysis method for boundary layer flow and heat transfer over a permeable flat plate in a Darcian porous medium with radiation effects," *Journal of the Taiwan Institute of Chemical Engineers*, vol. 45, no. 4, pp. 1217–1224, 2014.

[28] S. Saleem, S. Nadeem, M. M. Rashidi, and C. S. Raju, "An optimal analysis of radiated nanomaterial flow with viscous dissipation and heat source," *Microsystem Technologies*, vol. 25, no. 2, pp. 683–689, 2019.

[29] I. Khan, U. Shafquat, M. Y. Malik, and H. Arif, "Numerical analysis of MHD Carreau fluid flow over a stretching cylinder with homogenous-heterogeneous reactions," *Results in Physics*, vol. 9, pp. 1141–1147, 2018.

[30] V. Marinca, H. Nicolae, and N. Iacob, "Optimal homotopy asymptotic method with application to thin film flow," *Open Physics*, vol. 6, no. 3, pp. 648–653, 2008.

[31] O. D. Makinde and P. Oladapo Olanrewaju, "Buoyancy effects on thermal boundary layer over a vertical plate with a convective surface boundary condition," *Journal of Fluids Engineering*, vol. 132, no. 4, 2010.

[32] S. M. Ibrahim and N. B. Reddy, "Similarity solution of heat and mass transfer for natural convection over a moving vertical plate with internal heat generation and a convective boundary condition in the presence of thermal radiation, viscous dissipation, and chemical reaction," *International Scholarly Research Notices*, vol. 2013, 10 pages, 2013.